



Histone deacetylases maintain expression of the pluripotent gene network via recruitment of RNA polymerase II to coding and noncoding loci

Richard D.W. Kelly, Kristy R. Stengel, Aditya Chandru, et al.

Genome Res. published online January 30, 2024
Access the most recent version at doi:[10.1101/gr.278050.123](https://doi.org/10.1101/gr.278050.123)

P<P Published online January 30, 2024 in advance of the print journal.

Open Access Freely available online through the *Genome Research* Open Access option.

Creative Commons License This article, published in *Genome Research*, is available under a Creative Commons License (Attribution-NonCommercial 4.0 International), as described at <http://creativecommons.org/licenses/by-nc/4.0/>.

Email Alerting Service Receive free email alerts when new articles cite this article - sign up in the box at the top right corner of the article or [click here](#).

An advertisement banner with a teal background. On the left, the text reads "CRISPR and RNAi Genetic Screening. Your new superpower." In the center, there is a white-bordered box containing the words "LEARN MORE". On the right, there is a photograph of a woman wearing a red superhero mask and a red cape, and the Cellecta logo, which consists of a cluster of green dots.

To subscribe to *Genome Research* go to:
<https://genome.cshlp.org/subscriptions>

Research

Histone deacetylases maintain expression of the pluripotent gene network via recruitment of RNA polymerase II to coding and noncoding loci

Richard D.W. Kelly,¹ Kristy R. Stengel,² Aditya Chandru,³ Lyndsey C. Johnson,⁴ Scott W. Hiebert,^{5,6} and Shaun M. Cowley¹

¹Department of Molecular and Cell Biology, Henry Wellcome Building, University of Leicester, Leicester LE1 9HN, United Kingdom;

²Albert Einstein College of Medicine, Jack and Pearl Resnick Campus, Bronx, New York 10461, USA; ³Cancer Research UK Beatson

Institute, Bearsden, Glasgow G61 1BD, United Kingdom; ⁴Locate Bio Limited, MediCity, Beeston, Nottingham NG90 6BH, United Kingdom; ⁵Department of Biochemistry, Vanderbilt University School of Medicine, Nashville, Tennessee 37232, USA;

⁶Vanderbilt-Ingram Cancer Center, Vanderbilt University Medical Center, Nashville, Tennessee 37232, USA

Histone acetylation is a dynamic modification regulated by the opposing actions of histone acetyltransferases (HATs) and histone deacetylases (HDACs). Deacetylation of histone tails results in chromatin tightening, and therefore, HDACs are generally regarded as transcriptional repressors. Counterintuitively, simultaneous deletion of *Hdac1* and *Hdac2* in embryonic stem cells (ESCs) reduces expression of the pluripotency-associated transcription factors *Pou5f1*, *Sox2*, and *Nanog* (PSN). By shaping global histone acetylation patterns, HDACs indirectly regulate the activity of acetyl-lysine readers, such as the transcriptional activator BRD4. Here, we use inhibitors of HDACs and BRD4 (LBH589 and JQ1, respectively) in combination with precision nuclear run-on and sequencing (PRO-seq) to examine their roles in defining the ESC transcriptome. Both LBH589 and JQ1 causes a marked reduction in the pluripotent gene network. However, although JQ1 treatment induces widespread transcriptional pausing, HDAC inhibition causes a reduction in both paused and elongating polymerase, suggesting an overall reduction in polymerase recruitment. Using enhancer RNA (eRNA) expression to measure enhancer activity, we find that LBH589-sensitive eRNAs are preferentially associated with superenhancers and PSN binding sites. These findings suggest that HDAC activity is required to maintain pluripotency by regulating the PSN enhancer network via the recruitment of RNA polymerase II.

[Supplemental material is available for this article.]

Acetylation of lysine residues in histone tails is an essential post-translational modification (PTM), dynamically regulated by the opposing actions of histone acetyltransferases (HATs) and histone deacetylases (HDACs) (Verdin and Ott 2015). HDACs are generally considered to be transcriptional repressors (Nagy et al. 1997; Haberland et al. 2009; Kelly and Cowley 2013), because histone deacetylation increases inter-nucleosomal affinity and the association of N-terminal tails with negatively charged DNA, promoting chromatin compaction (Luger and Richmond 1998; Robinson et al. 2008). In addition, loss of histone acetylation prevents the binding of bromodomain-containing proteins, such as TAFII1 (Jacobson et al. 2000) and BRD4 (Kanno et al. 2004), which act as transcriptional coactivators. Among the 18 HDAC enzymes present within mammalian cells, HDAC1, HDAC2, and HDAC3 (class I HDACs) have well-described roles in regulating gene expression as the catalytic core of seven multiprotein complexes: SIN3, NuRD, CoREST, MiDAC, MIER and RERE (HDAC1 and HDAC2), and NCoR (HDAC3) (Millard et al. 2017). Each complex, with its unique arrangements of components, targets HDACs to specific genomic regions through the recognition of histones and interaction with transcription factors (Millard et al. 2017).

Despite a well-established role for HDACs in transcriptional repression, loss of HDAC activity, either through genetic deletion (Zupkovitz et al. 2006; Chen et al. 2013; Dovey et al. 2013; Jamaladdin et al. 2014; Stengel et al. 2017) or through HDAC inhibitors (HDACi) (Karantzali et al. 2008; Baltus et al. 2009; Kim et al. 2013; Greer et al. 2015; Gryder et al. 2019b; Baker et al. 2023), also reduces the expression of a subset of genes. In addition, HDAC activity is required for interferon-induced transcriptional initiation of the immediate-early genes (Chang et al. 2004; Sakamoto et al. 2004). In mammalian cells, HDACs are enriched at transcriptionally active enhancers, promoters, and gene bodies, suggesting an alternative and nonrepressive function (Wang et al. 2009; Kidder and Palmer 2012; Whyte et al. 2012). In tumor cells, HDAC inhibition reduced the activity of superenhancers (SEs) via aberrant hyperacetylation, causing down-regulation of SE-driven transcription of genes such as *Myc* (Gryder et al. 2019a,b). An influential study from Métivier et al. (2003) showed that activation of the *PS2* gene required cyclical acetylation/deacetylation for transcription initiation to occur. In this model, HDACs are hypothesized to function by resetting histone-acetylation at promoters between rounds of initiation (Métivier et al. 2003). In addition to initiation, HDAC activity is also required for normal transcriptional elongation (Kim et al. 2013; Greer et al. 2015). Treatment

Corresponding author: smc57@le.ac.uk

Article published online before print. Article, supplemental material, and publication date are at <https://www.genome.org/cgi/doi/10.1101/gr.278050.123>. Freely available online through the *Genome Research* Open Access option.

© 2024 Kelly et al. This article, published in *Genome Research*, is available under a Creative Commons License (Attribution-NonCommercial 4.0 International), as described at <http://creativecommons.org/licenses/by-nc/4.0/>.

of cells with HDACi caused increased global histone acetylation levels, resulting in mislocalization of the bromodomain containing 4 (BRD4) (Kim et al. 2013; Greer et al. 2015), an essential cofactor in the conversion of RNA polymerase II (RNAP II) from a paused-to-elongating state (Jang et al. 2005; Yang et al. 2005; Kanno et al. 2014; Arnold et al. 2021). These observations indicate HDACs positively regulate transcription through the precise regulation of histone acetylation patterns.

Embryonic stem cells (ESCs) are widely used to study the transcriptional networks required for pluripotency and tissue-specific differentiation in early embryos (for review, see Martello and Smith 2014). We have previously shown an essential role for HDAC1 and HDAC2 (HDAC1/2) in maintaining the expression of the critical pluripotency-associated transcription factors POU5F1, SOX2 and NANOG (Jamaladdin et al. 2014). Similar transcriptional changes are observed in ESCs treated with HDACi (Karantzali et al. 2008; Baltus et al. 2009) and bromodomain inhibitors (Di Micco et al. 2014; Liu et al. 2014; Horne et al. 2015; Gonzales-Cope et al. 2016; Finley et al. 2018). This is important mechanistically, because bromodomain containing proteins are readers and HDACs erasers of acetylated histones, the latter regulates levels and the former interprets the signal. To further understand the role of dynamic histone acetylation and HDACs in gene regulation, we have examined the molecular mechanisms by which HDACs and the bromodomain and extraterminal motif (BET) family (BRD2-4) maintain expression of the pluripotency-associated gene network.

Results

HDAC1/2 maintain ESC pluripotency in a gene dosage-dependent manner

We previously showed that conditional deletion of either *Hdac1* or *Hdac2* alone does not alter the expression of pluripotency-associated transcription factors in mouse ESCs (Dovey et al. 2010b). In contrast, double-knockout (DKO) of *Hdac1* and *Hdac2* caused a reduction in *Pou5f1* and *Nanog*, before a catastrophic loss of cell viability (Jamaladdin et al. 2014). ESCs that retain a single copy of *Hdac2* (*Hdac1*-KO; *Hdac2*-Het), on the other hand, are viable but have a significant reduction in the total deacetylase activity (Jamaladdin et al. 2014). To analyze the transcriptome in ESCs with differing levels of HDAC1/2 activity, we performed a comparative microarray analysis of DKO and *Hdac1*-KO; *Hdac2*-Het cells at 0 (Ctrl) and 3 d after deletion. It takes 4 d for HDAC1/2 to turnover completely, but this time point was chosen to attain the lowest possible amount of HDAC1/2 protein while still retaining cell viability in the DKO cells. Although there were numerous up-regulated transcripts following KO, consistent with a role in gene repression, there were also many genes whose activity was down-regulated by a reduction in HDAC activity. Both DKO and *Hdac1*-KO; *Hdac2*-Het ESCs revealed significantly (FDR<0.05) reduced expression of *Pou5f1*, *Nanog*, *Esrrb*, and *Phc1* (Fig. 1A). DKO cells also showed a reduction in additional pluripotency-associated factors, including *Klf4*, *Gdf3*, and *Sall1* (Fig. 1A, cf. upper and lower panels). Gene set enrichment analysis (GSEA) (Mootha et al. 2003; Subramanian et al. 2005) revealed both DKO and *Hdac1*-KO; *Hdac2*-Het cells showed a reduction in pluripotency-associated gene signatures compared with published pluripotent networks (Fig. 1B; Supplemental Fig. S1B). Importantly, reduced expression of pluripotent factors was not accompanied by an increase in differentiation markers (*Gata4*, *Fgf5*, or *Sox17*) (Supple-

mental Fig. S1A), indicating a direct requirement for deacetylase activity rather than a generalized response to ESC differentiation. To confirm that changes in mRNA were also reflected in protein levels, we examined NANOG and POU5F1 by western blotting. Upon simultaneous deletion of *Hdac1/2*, we observed a 5.5- and 3.4-fold reduction in NANOG and POU5F1 protein levels, respectively (Fig. 1C). In comparison, compound *Hdac1*-KO; *Hdac2*-Het ESCs expressed twofold less NANOG and POU5F1 (Fig. 1C), a smaller reduction than DKO cells, showing a gene-dosage effect of HDAC1/2 activity on pluripotent gene expression. HDAC3 is a highly related homolog of HDAC1/2 that regulates gene expression as a component of the NCoR1/SMRT complex (Watson et al. 2012). We used *Hdac3* conditional KO ESCs (Simandi et al. 2016) to address whether reduced expression of pluripotency-associated genes was a general consequence of class I HDAC loss. In contrast to HDAC1/2 DKO cells, cells lacking HDAC3 showed no significant change in *Esrrb*, *Klf4*, *Nanog*, or *Pou5f1* (Supplemental Fig. S1C). Taken together, these data show a positive role for HDAC1/2 in the expression of pluripotent factors in ESCs.

Acute HDAC inhibition attenuates pluripotency-associated gene expression without inducing differentiation

Investigating the mechanistic relationship between HDAC1/2 and pluripotency using KO models is challenging because the half-lives of HDAC1/2 are ~24 h, and it takes 3–4 d until the proteins turnover completely (Jamaladdin et al. 2014). Therefore, to evaluate the direct effects of HDAC activity on gene expression in ESCs, we treated E14 cells with the HDACi LBH589 (panobinostat) (Laubach et al. 2015). Because we sought to monitor rapid changes in transcription (at 2–6 h) a hydroxamic acid-based inhibitor was preferable owing to their fast-on/fast-off HDAC-binding kinetics, as opposed to the slow-on/tight-binding kinetics of more specific aminobenzamide inhibitors, for example, MS-275 (Chou et al. 2008; Beconi et al. 2012; Lauffer et al. 2013). To identify HDAC-dependent immediate early genes, we performed a comparative microarray analysis on mRNA isolated from ESCs treated with LBH589 at 2, 6, and 18 h compared with untreated controls. A similar proportion of genes showed increased and decreased expression at all time points, indicating HDAC activity has both positive and negative effects on transcription in ESCs (Fig. 2A). Consistent with the *Hdac1/2* DKO model, GSEA showed a reduction in pluripotency-associated gene signatures following treatment with LBH589 (Fig. 2B). Importantly, germ layer differentiation was not stimulated (Fig. 2C), again implying that reduced pluripotency was caused by a reduction in HDAC activity rather than as a consequence of differentiation. We observed reduced expression of *Sox2* as early as 2 h, with *Esrrb*, *Nanog*, and *Klf4* significantly down at 6 h and beyond (Fig. 2D). To confirm that these changes were a direct result of impaired transcription and to remove any confounding effects of mRNA half-life, we pulse-labeled ESCs with 5-ethynyl uridine (EU) to label and purify nascent mRNA, followed by RT-quantitative polymerase chain reaction (qPCR). In the presence of LBH589, nascent *Pou5f1* and *Nanog* transcripts decreased within 1 h of treatment and showed a progressive reduction at 2 and 6 h (Supplemental Fig. S2A). Together, these findings show that acute inhibition of HDAC activity in ESCs directly attenuates pluripotent gene expression without inducing cellular differentiation.

Histone acetylation correlates with active transcription in all eukaryotes (Barnes et al. 2019) and is dynamically regulated by HDAC enzymes. We, therefore, addressed the level of H3 Lys27 acetylation (H3K27ac) at the *Nanog* and *Pou5f1* promoters and

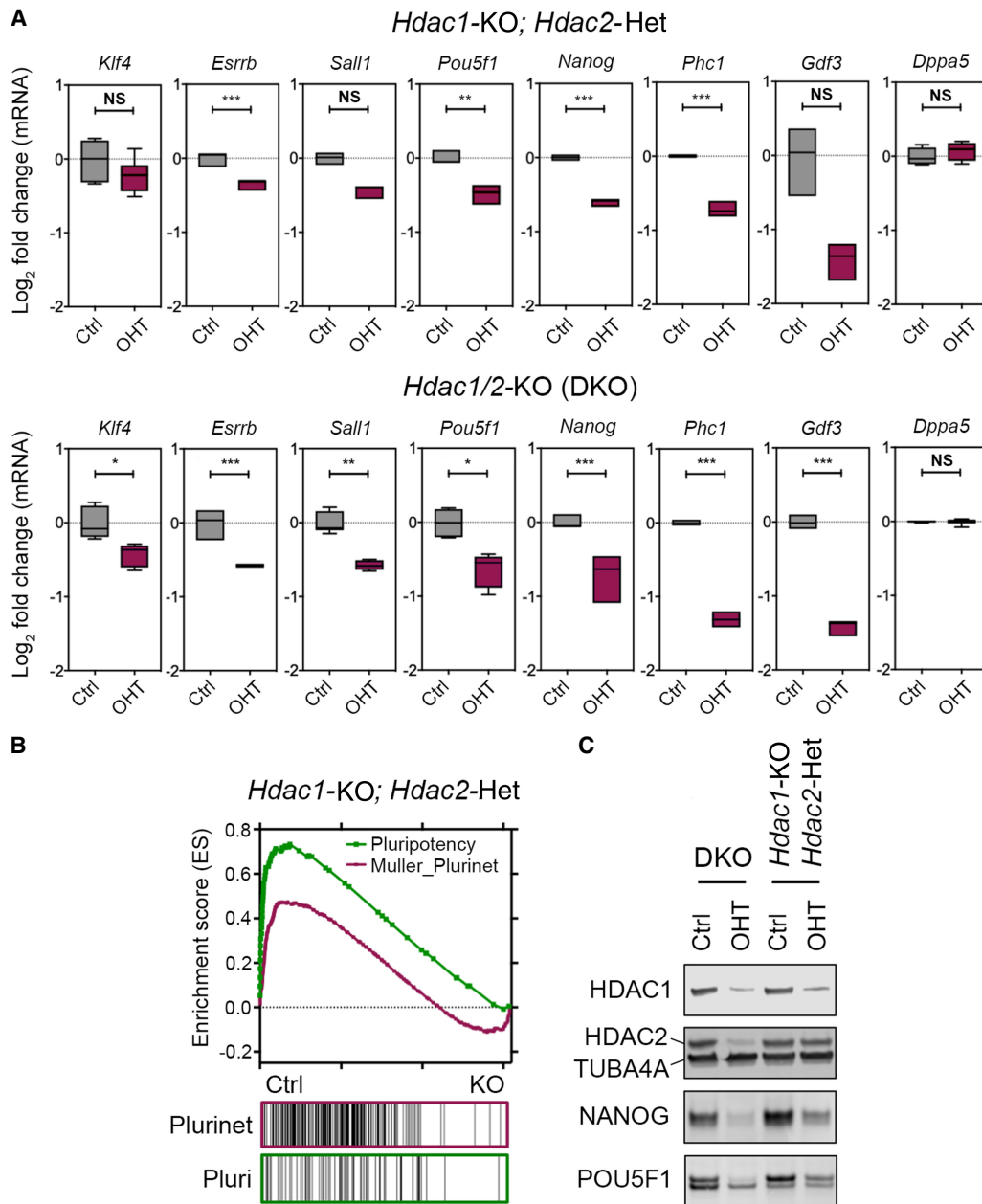


Figure 1. HDAC1 and 2 (HDAC1/2) maintain ESC pluripotency in a gene dosage–dependent manner. (A) Microarray data from $n = 3$ biological replicates showing relative expression (\log_2 fold-change) of indicated pluripotency-associated genes in *Hdac1/2*-KO (DKO) and *Hdac1*-KO; *Hdac2*-Het cells at 0 (Ctrl) and 3 d after deletion (OHT). (B) Gene set enrichment analysis (GSEA) plot of microarray data showing Ctrl samples are enriched for the Muller PluriNet (ES = 0.47; $P < 0.0001$) and pluripotency (ES = 0.70; $P < 0.0001$) gene sets compared with *Hdac1*-KO; *Hdac2*-Het KO cells. (C) Western blot data for HDAC1, HDAC2, NANOG, and POU5F1 proteins in *Hdac1/2*-KO (DKO) and *Hdac1*-KO; *Hdac2*-Het cells at 0 (Ctrl) and 3 d after deletion (OHT). Tubulin, alpha 4A (TUBA4A) was used as a protein loading control.

regulatory regions following HDAC inhibition using chromatin immunoprecipitation (ChIP)–qPCR. The addition of LBH589 stimulated a rapid increase of H3K27ac at *cis*-regulatory loci, including enhancers of both *Nanog* and *Pou5f1* (Supplemental Fig. S2B), but not at the promoters of developmentally regulated genes (*Gata2* and *Spink2*) in a similar time frame to the reduction in transcription. This is an intriguing result as it shows increased histone acetylation at transcriptionally down-regulated genes, suggesting that active turnover, as part of a transcriptional acetylation/deacetylation cycle (Métivier et al. 2003) or as the global pattern of histone

acetylation (Greer et al. 2015), is more important than the simple accumulation of acetylation at a particular locus.

LBH589 and JQI target the same subset of pluripotency-associated genes

It has been proposed that increasing global histone acetylation levels using HDACi can sequester the acetyl-lysine reader protein, BRD4, away from critical sites, thereby reducing transcriptional elongation (Greer et al. 2015). BRD4 knockdown (Liu et al. 2014)

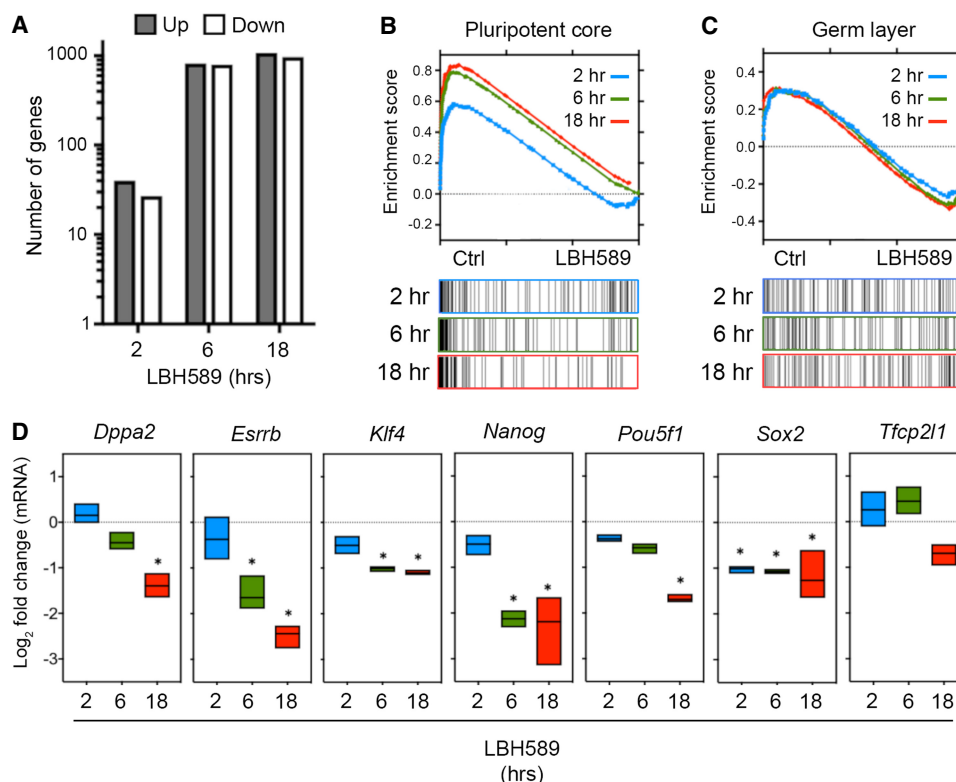


Figure 2. HDAC inhibition attenuates pluripotency-associated gene expression without inducing differentiation. (A) Microarray analysis: the number of genes differentially expressed (1.5-fold; FDR ≤ 0.05) at the indicated times following LBH589 treatment. (B) GSEA plot showing enrichment for the defined pluripotency gene set (Kim_Core_Module) in control versus LBH589-treated ESCs. LBH589 2 h (ES = 0.527; $P < 0.0001$), 6 h (ES = 0.789; $P < 0.0001$), and 18 h (ES = 0.83; $P < 0.0001$). (C) GSEA for Ctrl and LBH589 samples showed equal enrichment for the formation of the primary germ layer (GO:0001704; Germ Layer). (D) Microarray data from $n = 3$ biological replicates showing relative expression of indicated pluripotency-associated genes in ESCs treated with LBH589 for 2, 6, and 18 h. The statistical difference was calculated using Benjamini and Hochberg's false-discovery rate (FDR). Asterisk denotes significant changes in expression (≤ 1.5 -fold; FDR ≤ 0.05) relative to untreated control ESCs.

or inhibition using the bromodomain inhibitor JQ1 (Liu et al. 2014; Horne et al. 2015; Finley et al. 2018) has been reported to reduce the expression of pluripotent-associated factors. To explore the relationship between HDAC activity and BET family members (BRD2-4) in pluripotent gene expression, we treated ESCs with LBH589 (50 nM) and JQ1 (1 μ M) for 6 and 18 h. JQ1 treatment reduced the expression of *Nanog*, *Pou5f1*, *Sox2*, and *Esrrb* to a similar degree and in the same time frame as LBH589, suggesting that there may be a common mode of action (Fig. 3A). We reasoned that if BRD4 levels were limiting *Nanog* expression, overexpression of BRD4 would rescue the effects of HDAC inhibition. To test this hypothesis, we generated ESCs stably overexpressing BRD4 and, consistent with previous reports (Wu et al. 2015), observed a 4.6-fold increase in *Nanog* expression (Fig. 3B). However, treatment with LBH589 caused a 2.4-fold ($P < 0.0001$) and 1.7-fold ($P = 0.0241$) reduction in *Nanog* levels with or without additional BRD4, respectively (Fig. 3B). Taken together, these results indicate that sequestration of BRD4 can indeed limit *Nanog* expression, although the inability of additional BRD4 to rescue the effects of HDACi treatment suggests additional BRD4-independent roles for HDACs at pluripotency-associated genes.

HDAC inhibition causes increased expression of promoter upstream transcripts and a loss of promoter-proximal polymerase

To examine the roles of HDACs and BET family members in shaping the ESC transcriptome, we performed precision nuclear run-on

and sequencing (PRO-seq) analysis (Kwak et al. 2013). PRO-seq enables the quantification of nascent RNAs and transcriptionally engaged RNA polymerases across the genome, effectively an assay that combines the attributes of nascent RNA-seq with ChIP-seq for RNAP II. To remain consistent with previous experiments, we compared PRO-seq outputs for LBH589-treated cells at 2 h and 6 h and for JQ1 at 2 h. Although our study was primarily focused on the pluripotent gene network, we initially examined the role of HDACs from a global perspective. Analysis of RNAP II occupancies across the transcription start sites (TSS; ± 5 kb) of RefSeq-annotated genes showed significant differences in JQ1- and LBH589-treated cells (Fig. 4A). BRD4 promotes the conversion of proximally paused polymerases to an elongating form via the recruitment of P-TEFb (Jang et al. 2005; Yang et al. 2005). We observed a similar mechanism in our system, as 64% of JQ1-sensitive genes showed an increase in pausing (clusters A, B, and C) (Fig. 4B). Because LBH589 and JQ1 reduced the expression of pluripotency-associated genes (Fig. 3A), our expectation was that loss of deacetylase activity would affect RNAP II pausing in a similar fashion to JQ1. However, in contrast, the majority of genes in LBH589-treated cells showed a reduction in paused polymerase (clusters D, E, and F) (Fig. 4B). These data imply fundamental mechanistic differences in HDAC and BET family function. We also observed increased transcript levels upstream of the TSS in LBH589-treated cells, particularly at genes displaying increased gene body transcription (Fig. 4A,B; clusters C and D). In mammalian cells, active promoters

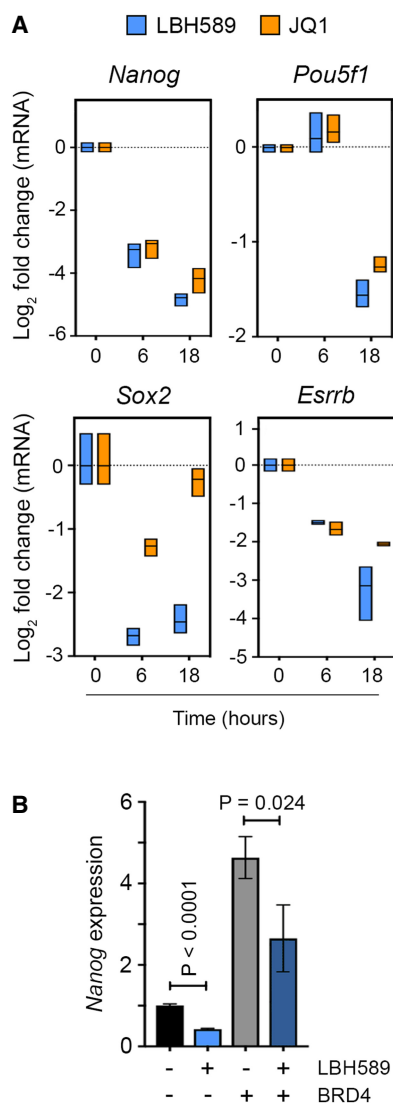


Figure 3. LBH589 and JQ1 target the same subset of pluripotency-associated genes and reduce BRD4 recruitment. (A) RT-qPCR analysis of pluripotency-associated gene expression following the treatment of ESCs with LBH589 or JQ1 for the indicated time points. Box plots represent the maximum expression range and mean from three biological replicates. (B) RT-qPCR analysis for *Nanog* expression in ESCs treated with LBH589 and/or overexpressing BRD4, as indicated. Values represent mean (\pm SEM) relative expression compared with the wild-type for $n=6$ biological replicates. Statistical differences were calculated using a paired Student's *t*-test.

generate short and unstable promoter upstream transcripts (PROMPTs) on the opposite strand to protein-coding genes (Preker et al. 2008). To examine the effects of HDAC inhibition on the generation of PROMPTs, we focused on genes whose expression is up-regulated by LBH589 treatment (clusters C and D). Metagene plots show that LBH589, but not JQ1, produced an increase in PROMPT levels (Fig. 4C). Examination of individual up-regulated genes, *Fos* and *Tp52* (Fig. 4D), emphasizes the level of increased transcription of PROMPTs following HDAC inhibition. These findings imply HDACs play a role in reducing PROMPT generation, either directly through RNAP II recruitment or indirectly through histone acetylation levels in the vicinity of the TSS.

HDAC activity is required for RNAP II recruitment to pluripotency-associated genes

Pluripotency is the defining phenotype of ESCs. Therefore, among a wide range of differentially expressed genes (4721 at 2 h with LBH589) (Fig. 4A), we chose to examine the pluripotency-associated gene network. We used our PRO-seq data to assess the role of HDACs in transcriptional pausing and elongation among the broader network of factors required for pluripotency. Transcription was reduced in 34 of 59 (2 h) and 45 of 59 (6 h) pluripotent network genes in LBH589-treated cells and 30 of 59 in cells with JQ1 (Fig. 5A), showing a direct requirement for both deacetylase activity and BET family members. Consistent with our initial microarray experiments (Fig. 2A), PRO-seq data showed similar numbers of highly expressed genes are up- and down-regulated with LBH589 (Supplemental Fig. S3), indicating that this is not a generic decrease in abundant transcripts. The reduction in transcription following JQ1 treatment is accompanied by a significant increase in the paused index (PI; the ratio of promoter-proximal to gene body transcript levels) (Fig. 5B; Kwak et al. 2013), indicating that reduced expression may be owing to an inability to resolve paused RNAP II. In contrast, HDAC inhibition produced no consistent change in PI among pluripotency-associated factors (Fig. 5B, cf. JQ1 with LBH589 at 2 and 6 h). Metagene plots of polymerase density among the pluripotent gene network (Fig. 5C) showed increased RNAP II pausing with JQ1, whereas LBH589 treatment caused a reduction in both promoter-proximal and gene body transcription. A reduction in both paused and elongating polymerase can be observed at individual genes such as *Nanog*, *Sox2*, and *Pou5f1* (Fig. 5D). An overall reduction in transcription suggests that HDAC activity may be required for optimal RNAP II recruitment. To test this further, we performed ChIP-qPCR for RNAP II at the *Nanog*, *Klf4*, and *Pou5f1* promoters in the presence or absence of LBH589 (Fig. 5E). We observed reduced RNAP II binding at all three genes when treated with LBH589 compared with controls, whereas there was no change with JQ1. Taken together, these findings show that HDAC inhibition reduced the level of both paused and elongating polymerase at pluripotency-associated genes, consistent with a role in RNAP II recruitment that appears to be mechanistically independent of BRD4.

HDACs positively regulate a subset of enhancers associated with the pluripotent gene network

Analysis of PRO-seq data using nascent RNA sequencing analysis (NRSA) (Wang et al. 2018) identified transcripts in intergenic regions corresponding to enhancer RNAs (eRNAs). Because eRNA levels are a more sensitive indicator of enhancer activity than the histone modifications (Kim et al. 2010), we can directly infer the effects of LBH589 and JQ1 on enhancer activity from their transcription. We observed, consistent with changes in mRNA levels (Fig. 2A), a similar number of down- (199) and up-regulated (149) eRNAs following a 2-h LBH589 treatment, with an increasing number (627 down and 539 up) at 6 h (Fig. 6A). In contrast, the addition of JQ1 predominantly down-regulated eRNAs (1196 down vs. 33 up) and overall affected a far greater number of eRNAs than did LBH589. These data indicate that BET family members play an important role in the expression of eRNAs and that this is independent of HDAC activity.

Both BRD4 (Di Micco et al. 2014) and HDACs (Sanchez et al. 2018) are known to alter transcriptional dynamics at SEs. Therefore, we examined the transcription of eRNAs that overlap with SEs in ESCs treated with either LBH589 or JQ1. A greater

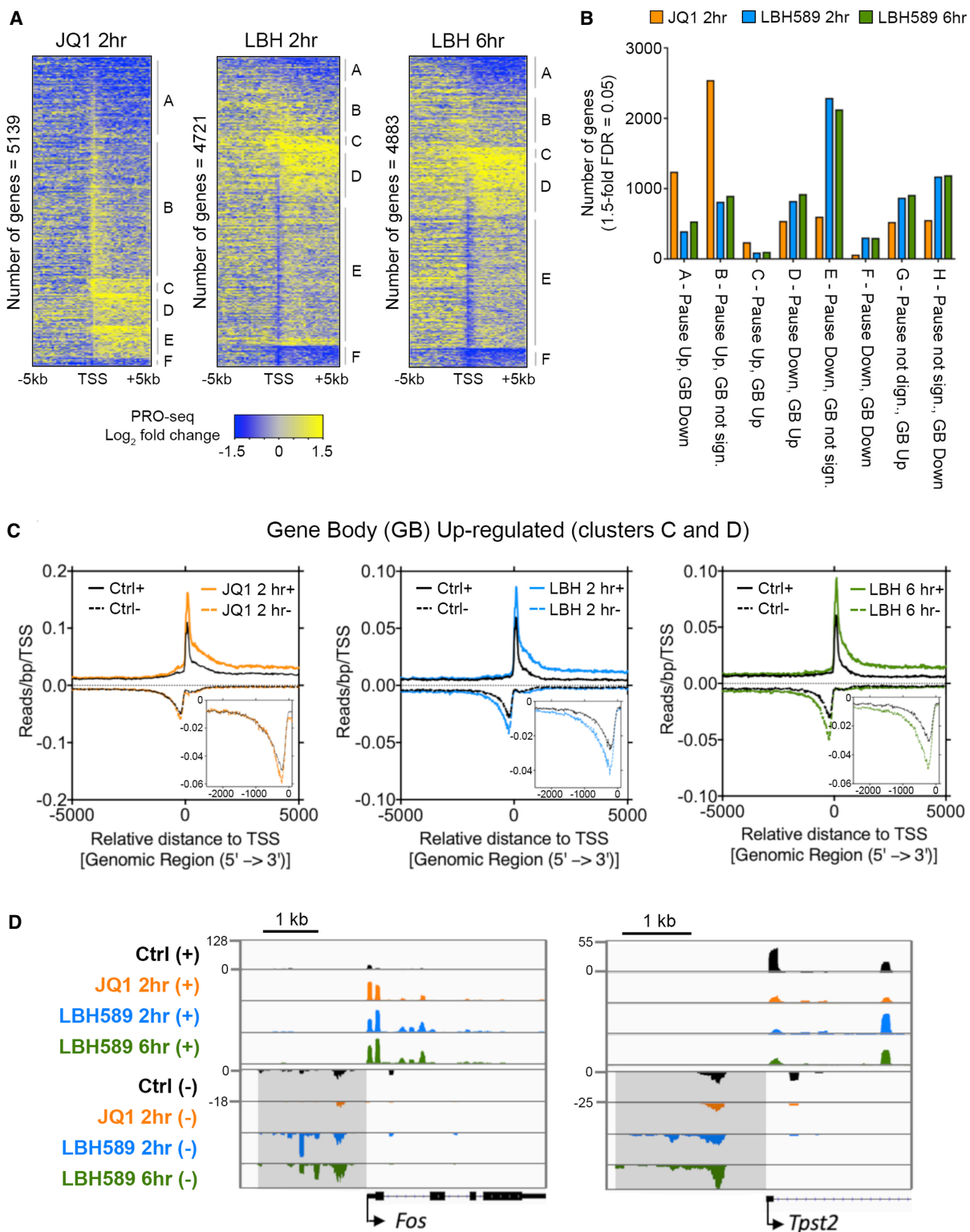


Figure 4. HDAC inhibition causes increased expression of promoter upstream transcripts (PROMPTs) and a loss of promoter-proximal polymerase. (A) Heatmaps displaying a log₂-fold change of PRO-seq read counts in 200-bp bins (TSS ± 5 kb) at RefSeq genes displaying increased or decreased pause index changes following JQ1 (2 h) or LBH589 (2 h and 6 h) treatment. Genes were ranked based on the log₂-transformed fold-change of RNA polymerase in the promoter-proximal region. (B) A number of gene clusters (A–H) with similar transcriptional changes are shown. For each treatment, genes were clustered based on change (±1.5-fold; FDR ≤ 0.05) in gene body or paused index changes. (C) Metagenes plots (TSS ± 5 kb) of RNAP II densities at genes showing increased gene body levels following the treatment with JQ1 or LBH589. *Insets* show increased antisense transcripts (PROMPTs) relative to TSS in greater detail. (D) PRO-seq Integrative Genomics Viewer (IGV; Robinson et al. 2011) bedGraph screenshots of *Fos* and *Tpst2* TSS with control, JQ1, or LBH589 treatments for the indicated times. Shaded areas indicate increased antisense transcription in LBH589-treated samples.

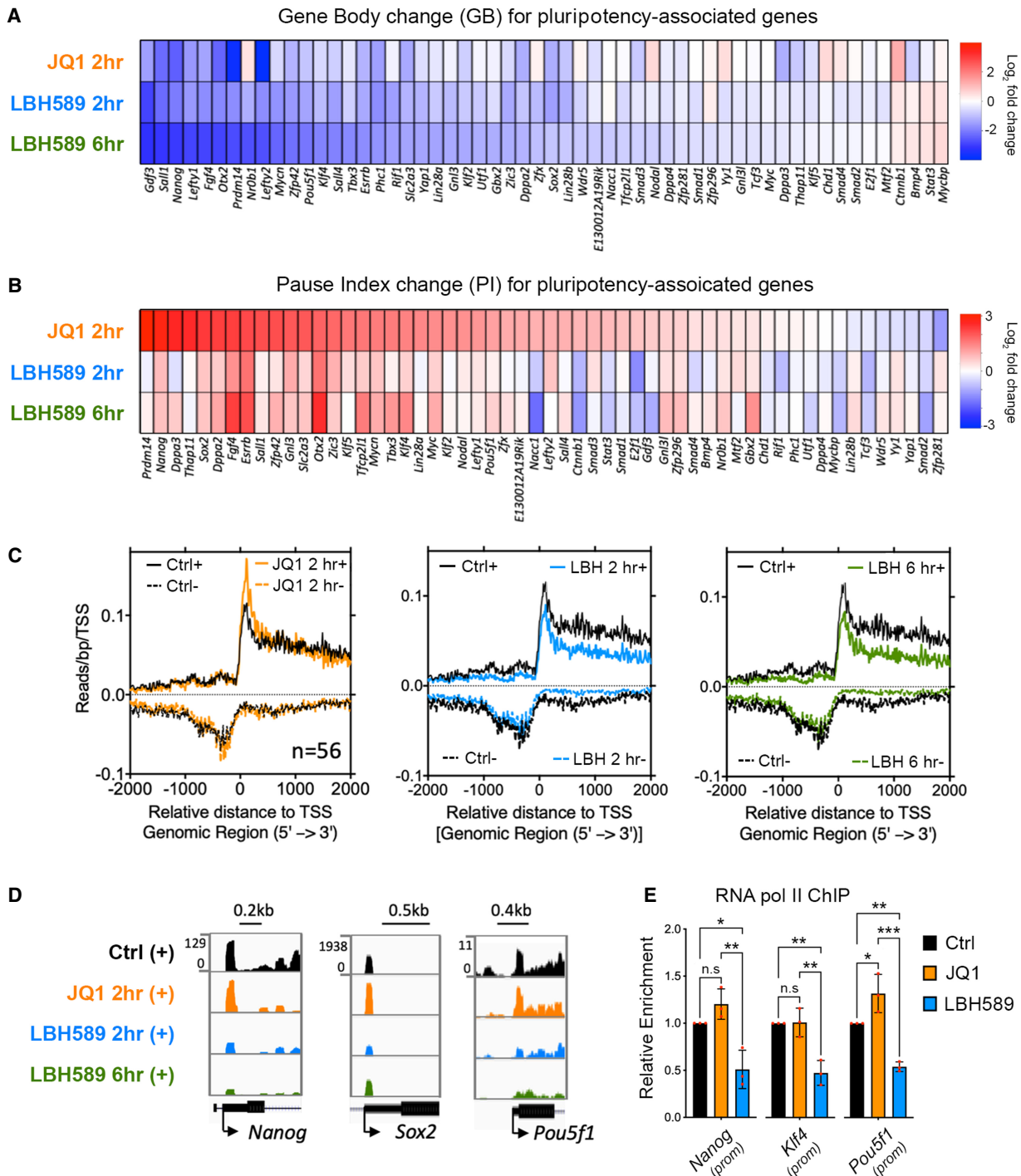


Figure 5. HDACs are required for expression of the pluripotent gene network via recruitment of RNA polymerase II (RNAP II). (A) PRO-seq analysis displaying the effects of JQ1 or LBH589 treatment on the level of gene body transcripts for pluripotent gene network members. Heatmap shows the log₂ fold-change relative to untreated controls. (B) Heatmap shows the effects of JQ1 and LBH589 treatment on the pausing index (the ratio of promoter-proximal to gene body transcript levels) changes relative to untreated controls. (C) Metagenic plots (TSS ± 2 kb) of pluripotency-associated genes showing reduced initiation and elongation in LBH589-treated samples. (D) RNAP II density at *Nanog*, *Sox2*, and *Pou5f1* TSS in either control or JQ1- or LBH589-treated ESCs. (E) ChIP-qPCR for RNAP II at the indicated promoters in either control or JQ1- or LBH589-treated (2 h) ESCs. Bars represent the mean (±SEM) of n = 3 biological replicates. (*) P < 0.05, (**) P < 0.01, (***) P < 0.001, (n.s.) not significant.

proportion of the eRNAs down-regulated by LBH589 overlapped with SEs (39 of 199, 20%) than those with JQ1 (57 of 1199, 5%) (Supplemental Fig. S4). Examination of individual SEs (*Nanog*,

Mycn, and *Phc1*) shows a distinct reduction in transcription upon HDAC inhibition that appeared unaffected by JQ1 treatment (Fig. 6B, cf. orange and blue/green peaks in shaded regions).

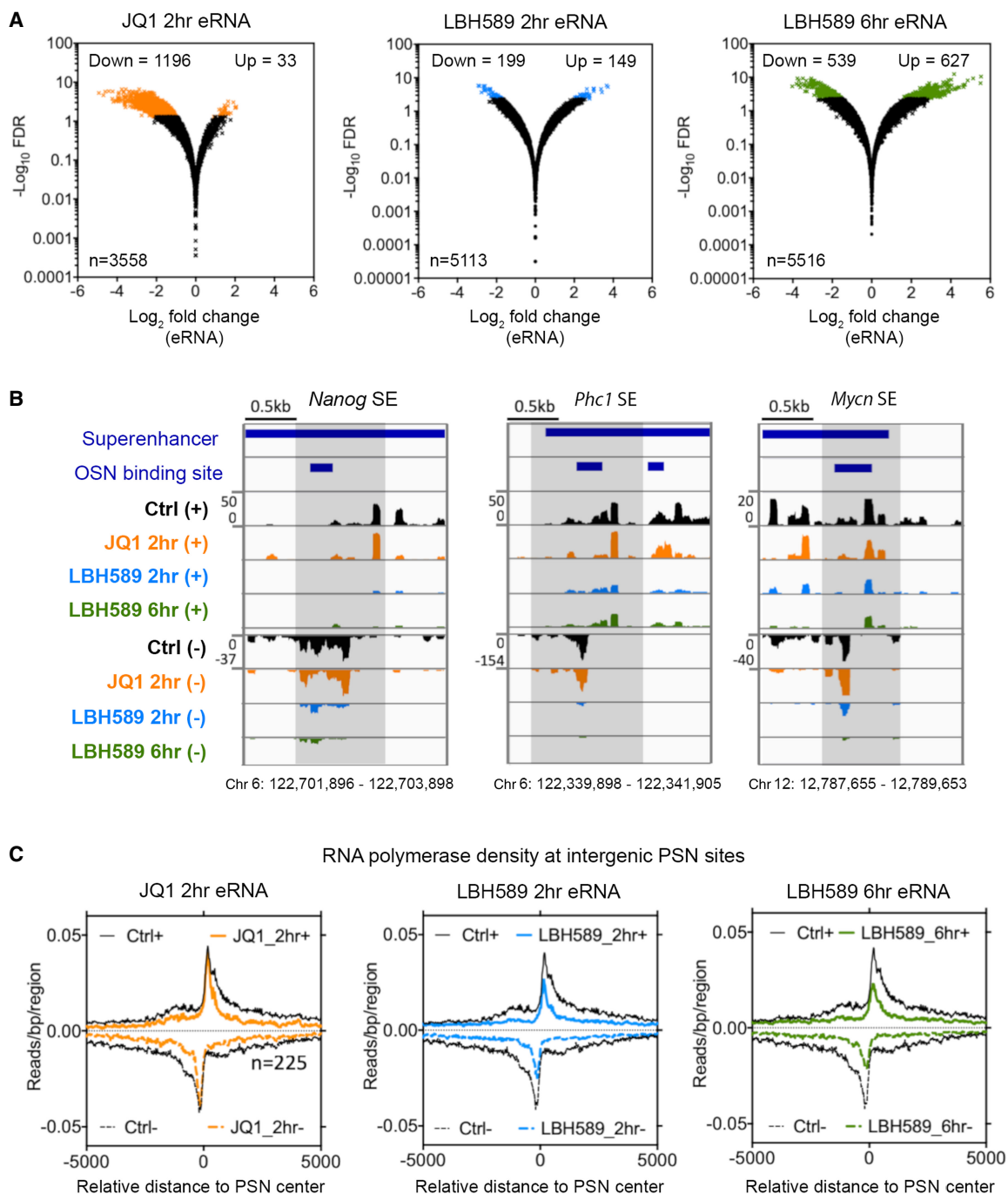


Figure 6. HDACs positively regulate a subset of eRNAs associated with superenhancers (SEs). (A) Volcano plot showing changes in eRNA transcription following treatment with JQ1 or LBH589 for the indicated time points. Statistically enriched (± 1.5 -fold; $FDR \leq 0.05$) eRNA transcripts are indicated in orange, blue, and green. (B) IGV genomic tracks of PRO-seq RNAP II densities at intergenic POU5F1/SOX2/NANOG (PSN) binding sites associated with the indicated SE regions. Shaded areas indicate regions of decreased transcription following LBH589 treatment. (C) Metagene plots of RNAP II density at intergenic PSN binding sites following the indicated treatments.

Because SEs are defined in part by increased recruitment of lineage-specific transcription factors, we hypothesized that HDAC activity may be required for eRNAs associated with the core pluripotency-associated transcription factors POU5F1, SOX2, and NANOG (PSN). We performed an unbiased analysis of eRNA transcription at all PSN binding sites. Upon HDAC inhibition, we observed a re-

duction in RNAP II density at both the TSS and the body of the transcript, indicating a reduction in recruitment, whereas JQ1 predominantly affected elongation (Fig. 6C). These data suggest that within 2 h of LBH589 treatment, enhancers associated with PSN function have reduced activity, contributing to the decrease in expression of the entire pluripotent gene network (Fig. 5A).

Discussion

HDAC enzymes and their associated complexes (e.g., SIN3A) are generally viewed as negative regulators of gene expression. The removal of acetyl groups from histone tails leads to a tightening of chromatin that prevents binding of transcription factors. Moreover, transcriptionally silent regions of the genome generally contain hypoacetylated histones (Barnes et al. 2019 and references therein). Despite this, there are several lines of evidence that indicate that HDACs play a role in active transcription. ChIP experiments for class I HDACs indicate that they are recruited to both enhancers and promoters of active genes (Wang et al. 2009; Kidder and Palmer 2012; Whyte et al. 2012). Acetylation/deacetylation cycling may be required to reset promoters between rounds of initiation (Métivier et al. 2003). The latter results have only been shown in a limited number of genes, but the concept is supported by the dynamic turnover of histone acetylation. Acetylation sites within the H2B tail are subject to rapid deacetylation with a half-life of ~10 min (Weinert et al. 2018). Although these data all support a role in transcription, the readout of histone acetylation remains highly dependent on genomic context, because HDAC inhibition results in both up- and down-regulated genes (Dovey et al. 2010a).

In ESCs, we have shown that HDAC1/2 (Fig. 1A), but not HDAC3 (Supplemental Fig. S1C), are required for expression of the pluripotent gene network. This activity is dependent on gene dosage because a hypomorphic *Hdac1*-KO; *Hdac2*-Het cell line has an intermediate level of *Pou5f1* and *Nanog* expression compared with single (Dovey et al. 2010b) or DKO ESCs (Fig. 1A; Jamaladdin et al. 2014). HDAC1/2 are incorporated into six biochemically and functionally distinct multiprotein complexes: SIN3, NuRD, CoREST, MiDAC, MIER, and RERE (Kelly and Cowley 2013; Millard et al. 2017). ESCs in which the NuRD (Kaji et al. 2006; Burgold et al. 2019), CoREST (Foster et al. 2010), and MiDAC (Turnbull et al. 2020) complexes are perturbed still retain pluripotency. In contrast, knockdown of *Sin3a* (Saunders et al. 2006; Fazio et al. 2008; Baltus et al. 2009; Adams et al. 2018; Zhu et al. 2018) or SIN3A complex components (Streubel et al. 2017) reduced the expression of *Nanog* and other pluripotency-associated factors, suggesting that the Sin3 complex may be the critical HDAC1/2 complex component.

Although *Hdac1/2* double-knockout ESCs show a robust decrease in *Nanog* transcription (Fig. 1A), the stable nature of class I HDACs (half-life of 24 h) obliged us to use HDACi to examine the direct effects of deacetylation on transcription. Analysis of nascent transcripts in ESCs showed a significant reduction in *Nanog* and *Pou5f1* transcription within 2 h of LBH589 treatment (Supplemental Fig. S2A). The similarity between LBH589 treatment (a general inhibitor of Zn²⁺-dependent HDACs) and *Hdac1/2* DKO cells suggests that this acute decrease in pluripotency-associated factors is a result of HDAC1/2 inhibition. A critical role of HDAC1/2 in ESCs is to regulate histone acetylation levels (e.g., H3K18ac) across the genome (Kelly et al. 2018), thereby indirectly affecting the recruitment of acetyl-lysine readers, such as BRD4. Increased histone acetylation across the genome could potentially sequester a limiting pool of BRD4 from critical promoters, resulting in a reduced transcription (Greer et al. 2015). In ESCs, we find that overexpression of BRD4 increased the level of *Nanog* expression, indicating that it is limiting (Fig. 3B). However, overexpression of BRD4 was insufficient to rescue the decrease in *Nanog* transcription upon HDAC inhibition, arguing in favor of the collaborative but independent roles of BRD4 and HDACs.

To examine the direct roles of HDACs and BET family members (BRD2-4), we performed PRO-seq in ESCs treated with both LBH589 and the bromodomain inhibitor JQ1 (Fig. 4). PRO-seq allows high-resolution mapping of active RNA polymerases across the genome at both coding and noncoding regions and provides information on both the abundance and directionality of transcripts. Analysis of the transcriptome in LBH589-treated ESCs revealed that the majority of genes in LBH589-treated cells showed a reduction in paused polymerase (Fig. 4B, clusters D, E, and F). This contrasts with the addition of JQ1, which produced a significant increase in paused polymerase (Fig. 4B, cluster B), implying fundamental mechanistic differences in HDAC and BET family function. Vaid et al. (2020) performed an analogous PRO-seq study using trichostatin A in *Drosophila* S2 cells and found that up-regulated genes shared a high degree of pausing, suggesting a release of RNAP II in response to HDAC inhibition. However, it should be noted that our PRO-seq experiments used much longer treatment periods (2 and 6 h) than the Vaid et al. (2020) study (10 and 30 min), resulting in a greater number and variety of dysregulated genes.

RNAP II recruitment to promoters is the principal function of enhancers. Because enhancer activity is associated with the production of eRNAs, whose levels are correlated with the activity of neighboring genes (Andersson et al. 2014; Core et al. 2014), we used our PRO-seq data to examine the contribution of HDACs and BET family members to enhancer function in ESCs (Fig. 6A). JQ1 treatment reduced the transcription of 1196 eRNAs compared with only 199 with LBH589. However, the LBH589-sensitive eRNAs contained a far greater proportion of eRNAs associated with SE activity (Supplemental Fig. S4). The directionality of transcripts identified by PRO-seq also allows the identification of subenhancers contained with SEs. Examination of individual SEs, such as the *Nanog*, *Phc1*, and *Mycn*, shows an overall reduction in transcripts and RNAP II recruitment at each of the subenhancers within these regions (Fig. 6B).

Although our study has identified a role for HDACs in the activity of SEs in ESCs, there is accumulating evidence for their role in the maintenance of SEs in other cell types. Treatment of the human colon tumor cell line HCT116 with the natural HDACi, largazole, resulted in a reduction in RNAP II recruitment to the *MYC* SE (Sanchez et al. 2018). Moreover, reduced polymerase recruitment was independent of H3K27ac levels, although it remains possible that alternative sites of histone acetylation might be involved (Sanchez et al. 2018). The requirement of HDAC1/2 activity for *Myc* expression was also confirmed in pancreatic cancer (Stojanovic et al. 2017). In an elegant set of experiments, Gryder et al. (2019b) used constitutive and SE-driven reporters to identify classes of histone-modifying enzymes that preferentially affect SE-driven transcription in alveolar rhabdomyosarcoma cells. They discovered that compared with a variety of bromodomain inhibitors, including JQ1, SEs were more responsive to HDACi (Gryder et al. 2019b). Subsequently, they showed that HDAC inhibition triggers hyperacetylation-induced erosion of SE boundaries, which alters 3D chromatin dynamics and reduces RNAP II occupancy at specific gene loci (Gryder et al. 2019a). In ESCs, we observed an analogous reduction in transcriptionally engaged RNAP II at SEs following LBH589 treatment (Fig. 6B), providing evidence of a broader mechanistic requirement for HDAC activity in different cell types.

Transcription factors that define a cell-specific transcriptional program (such as POU5F1 and NANOG) have increased clusters of binding sites at cell type-specific SEs, which in turn, regulate their

own expression (Whyte et al. 2013). This self-reinforcing auto-regulatory network creates a system whereby loss of activity (e.g., treatment with HDACi) leads to a “self-reinforcing” collapse (Gryder et al. 2019b). This hypothesis would fit with our data in ESCs, which showed a reduction in eRNAs associated with PSN binding sites following LBH589 treatment (Fig. 6C). Because POU5F1/SOX/NANOG regulate their own genes, reduction in their protein levels following HDAC inhibition will naturally lead to reduced binding of these factors to their response elements, as well as a general reduction in transcription across the pluripotent gene network (Fig. 5A). In total, we found 4721 differentially expressed genes following 2-h LBH589 treatment (Fig. 4A), indicating that there are additional gene networks to be mined from this data set. Although it has been clear for some time that HDAC inhibition results in both the up- and down-regulation of genes (Clayton et al. 2006; Smith 2008), we have exploited the greatly increased temporal resolution of PRO-seq to begin to unravel the mechanistic basis for these changes in gene expression as a result of perturbing the dynamic regulation of histone acetylation.

Methods

ESC culture and stable BRD4-expressing lines

All mouse E14 ESCs (*Hdac1*^{L/L}, *Hdac1*^{L/L}; *Hdac2*^{L/wt} and *Hdac3*^{L/L}) were cultured as previously described by Jamaladdin et al. (2014). The piggyBAC-BRD4 expression construct was generated by the PROTEX facility at the University of Leicester (<https://le.ac.uk/mcb/facilities-and-technologies/protex>). The BRD4 cDNA was amplified by PCR, subcloned into pLEICS-38 using the appropriate homology sequences with an in-fusion cloning kit (Takara Bio), and then verified by sequencing (Addgene 83777). The resultant plasmid was transfected into 5 × 10⁵ E14-ESC along with transposase using Lipofectamine 2000. After 24 h after transfection, cells were cultured at low density (5000 cells/10-cm plate) and treated with 200 µg/mL G418 (Thermo Fisher Scientific) in ESC media for 10 d. G418-resistant single colonies were selected, expanded individually, and characterized for FLAG expression by western blotting.

Protein extraction and western blotting

Whole-cell extracts were prepared in cell lysis buffer containing 150 mM NaCl, 50 mM Tris-HCL (pH 7.5), 0.5% IEGPAL, and a protease inhibitor cocktail for 30 min at 4°C. Samples were cleared at 20,000g for 15 min, and the supernatant was used for the examination of soluble proteins. Histones were extracted from the insoluble pellet fraction using 0.4 N sulfuric acid overnight at 4°C. Proteins (30 µg) were resolved using SDS/PAGE and nitrocellulose membranes and were probed with the appropriate antibodies (Supplemental Table S1). The Odyssey infrared imaging system was used to quantify protein signals using the appropriate IR-dye conjugated secondary antibodies (LI-COR Biosciences).

Chromatin immunoprecipitation

ChIP for histone modifications was processed previously as described by Kelly et al. (2018). ChIP for transcription factors was processed by cross-linking cells with 1% formaldehyde for 10 min before being quenched in 125 mM glycine for 5 min. Cross-linked samples were then lysed for 5 min at 4°C in X-ChIP Buffer 1 (50 mM HEPES-KOH at pH 7.5, 140 mM NaCl, 1 mM EDTA, 10% glycerol, 0.5% NP-40, 0.25% Triton X-100, and a protease inhibitor cocktail), before being centrifuged at 900g for 5 min (4°C) and resuspended in X-ChIP buffer 2 (10 mM Tris-HCL at pH 8.0, 200 mM NaCl, 1 mM EDTA, 0.5 mM EGTA, and protease in-

hibitors) for 5 min at 4°C. Samples were then pelleted (900g for 5 min at 4°C) and resuspended in sonication buffer (10 mM Tris-HCL at pH 8.0, 100 mM NaCl, 1 mM EDTA, 0.5% EGTA, 0.1% Na-deoxycholate, 0.5% N-laurylsarcosine, 0.1% SDS, and protease inhibitors). Samples were sonicated for 4 min (20 sec on, 40 sec off) using a Bioruptor Pico (Diagenode). After sonication, samples were cleared with 1% Triton X-100 and pelleted (16000g for 5 min at 4°C). Chromatin was immunoprecipitated using 8 µg anti-H3K27ac (Active Motif 39133), 10 µL anti-BRD4 (Bethyl Laboratories A301-985A1), or 10 µL anti-RNAP II (Active Motif 39097) conjugated to 50 µL Dynabeads Protein G overnight at 4°C. A list of the antibodies used can be found in Supplemental Table S1. Beads were washed for 5 min in wash buffer A (50 mM Tris-HCL at pH 7.5, 10 mM EDTA, 75 mM NaCl), wash buffer B (50 mM Tris-HCL at pH 7.5, 10 mM EDTA, 125 mM NaCl), and wash buffer C (50 mM Tris-HCL at pH 7.5, 10 mM EDTA, 175 mM NaCl). DNA was purified using IPure kit v2 (Diagenode) according to the manufacturer's instructions.

RNA extraction and qPCR

Total RNA was isolated using TRIzol (Thermo Fisher Scientific) and Direct-zol RNA Kit (Zymo Research) according to the manufacturer's conditions. Samples were treated with DNase to remove genomic contamination. Five hundred nanograms of RNA was reverse-transcribed using 4 µL Q-Script cDNA SuperMix (Quanta Bioscience) in a 20-µL reaction according to the manufacturer's conditions. cDNA was diluted one in five with DNase- and RNase-free water. For each qPCR reaction, 2 µL of diluted cDNA or ChIP-DNA was amplified in 10-µL reactions containing 2× SensiMix (Bioline) and 1 µM of forward and reverse primers. A complete list of primer pairs, sequences, and annealing temperatures used in the study can be found in Supplemental Table S2. Reactions were performed on a Bio-Rad CFX-Connect under the following conditions: initial denaturation for 10 min at 94°C, followed by 40 cycles for 10 sec at 94°C, primer-specific annealing for 20 sec, and 5 sec at 72°C. Primer efficiency was calculated using absolute quantification from a standard curve. Where applicable statistical differences were identified using a paired two-tailed Student's *t*-test (Prism v7, GraphPad).

Microarray analysis

Comparative gene expression profiles were generated using the Illumina mouseWG-6, ver.2 (LBH589 and *Hdac1*^{L/L}; *Hdac2*^{L/wt}) or Agilent SurePrint G3 Mouse Gene Expression v2 8 × 60 K microarray (*Hdac3*^{L/L}) according to the manufacturer's instructions. Quality control of total mRNA was performed using a 2100 Bioanalyzer (Agilent), and only RNA integrity numbers (RIN) of eight or higher were selected for processing and array hybridization. LBH589 and *Hdac1*^{L/L}; *Hdac2*^{L/wt} arrays were analyzed using Partek Genomics Suite (Partek). GSEA (Subramanian et al. 2005) was performed using GSEA software, version 2.

Precision nuclear run-on assay (PRO-seq)

Nuclear run-on and library construction were performed as previously described (Kwak et al. 2013; Zhao et al. 2016). Briefly, 2 × 10⁷ nuclei were isolated following drug treatments performed in biological replicates. Nuclear run-ons were performed in the presence of 375 µM GTP, ATP, UTP, and biotin-11-CTP with 0.5% sarkosyl for 3 min at 30°C. Total RNA was isolated by TRIzol extraction and hydrolyzed in 0.2 N NaOH, and nascent RNAs were isolated by streptavidin bead binding (Dynabeads MyOne streptavidin T1 magnetic beads, Thermo Fisher Scientific). Following 3' adapter ligation, 5' cap removal and triphosphate repair, 5' hydroxyl repair,

and 5' adapter ligation, RNA was reverse-transcribed, and libraries were amplified. Following PAGE purification, PRO-seq libraries were provided to Vanderbilt Technologies for Advanced Genomics (VANTAGE) for sequencing (Illumina NextSeq 500 SE-75).

Analysis of PRO-seq data, including eRNA analysis, was performed using the NRSA pipeline using alignment files in the BAM format as input (Wang et al. 2018). Adapter trimming was conducted with Trimomatic-0.32 (Bolger et al. 2014) before alignment to mm10 (*Mus musculus*) genome build using Bowtie 2 (Langmead and Salzberg 2012). All reads <10 bp and ribosomal RNA reads were moved before inputting BAM files in to the NRSA pipeline. Transcriptional rates for genes were determined as follows: Promoter-proximal regions were determined by identifying the largest number of reads in a 50-bp window within ± 500 bp from known TSSs; gene body regions were identified within +0.5 kb downstream from a TSS to its transcription termination site (TTS); and pausing indexes were calculated by the ratio of promoter-proximal read density over gene-body read density. For enhancer analysis, NRSA identifies intergenic enhancers as paired bidirectional transcripts having a gap <400 bp between their 5' ends. Enhancer centers are defined as the midpoints of 5' end pairs. Transcripts within ± 2 kb of any annotated RefSeq gene are excluded from enhancer calling. Down-regulated eRNA overlapping with mouse ESC SE regions were identified using the overlapBed function in BEDTools (Quinlan and Hall 2010). BED files and coordinates for mouse ESC SEs were converted to mm10 genome build using the UCSC liftOver tool.

Metagene plots of nascent RNA levels around regions of interest were generated using the annotatePeaks.pl function in HOMER (<http://homer.ucsd.edu/homer/ngs/groseq/groseq.html>). POU5F1-SOX2-NANOG (PSN) binding sites were downloaded from and converted to mm10 genome build using the UCSC liftOver tool. Coordinates for TSSs of pluripotency-associated genes, or genes up-regulated following LBH589 treatment, were obtained from UCSC genome (<https://genome.ucsc.edu>). Average PRO-seq reads around these regions of interest (TSS ± 2 kb or 5 kb) were determined at 25-bp resolution and plotted as histograms in GraphPad Prism version 7 (<https://www.graphpad.com/scientific-software/prism/>).

SE analysis

Mouse ESC SEs (Whyte et al. 2013) and PSN binding sites (Chen et al. 2008) were converted to the mm10 genome build using the UCSC liftOver tool. BEDTools were then used to identify overlap between SEs and changes in eRNA levels following either LBH589 or JQ1 treatments.

Data access

All raw and processed microarray and sequencing data generated in this study have been submitted to the NCBI Gene Expression Omnibus (GEO; <https://www.ncbi.nlm.nih.gov/geo/>) under the accession number GSE136621.

Competing interest statement

The authors declare no competing interests.

Acknowledgments

We thank Prof. Ian Eperon, Dr. David English, Dr. Grace Adams, India-May Baker, and Donovan Lim for critical reading of the manuscript. We thank Dr. Nicolas Sylvius and the NUCLEUS Genomics facility for help with performing the microarray data collection; data analysis was assisted by Dr. Matthew Blades. Plasmid con-

structs were generated by the University of Leicester PROTEX facility. S.M.C. was supported by a senior nonclinical fellowship from the Medical Research Council (MRC; MR/J009202/1) and Biotechnology and Biological Sciences Research Council (BBSRC) project grants (BB/N002954/1, BB/P021689/1). S.W.H. was supported by grants from the Division of Cancer Prevention, National Cancer Institute (NIH; CA164605, CA64140).

Author contributions: R.D.W.K. designed and performed wet-laboratory experiments and conducted bioinformatics analysis. K.R.S. designed and performed wet-laboratory experiments and conducted bioinformatics analysis. A.C. performed bioinformatic analysis of the data. L.C.J. performed functional assays. S.W.H. designed the study and analyzed data. S.M.C. designed the study and wrote the manuscript with input from all coauthors.

References

- Adams GE, Chandru A, Cowley SM. 2018. Co-repressor, co-activator and general transcription factor: the many faces of the Sin3 histone deacetylase (HDAC) complex. *Biochem J* **475**: 3921–3932. doi:10.1042/BCJ20170314
- Andersson R, Gebhard C, Miguel-Escalada I, Hoof I, Bornholdt J, Boyd M, Chen Y, Zhao X, Schmidl C, Suzuki T, et al. 2014. An atlas of active enhancers across human cell types and tissues. *Nature* **507**: 455–461. doi:10.1038/nature12787
- Arnold M, Bressin A, Jasnovidova O, Meierhofer D, Mayer A. 2021. A BRD4-mediated elongation control point primes transcribing RNA polymerase II for 3'-processing and termination. *Mol Cell* **81**: 3589–3603.e13. doi:10.1016/j.molcel.2021.06.026
- Baker IM, Smalley JP, Sabat KA, Hodgkinson JT, Cowley SM. 2023. Comprehensive transcriptomic analysis of novel class I HDAC proteolysis targeting chimeras (PROTACs). *Biochemistry* **62**: 645–656. doi:10.1021/acs.biochem.2c00288
- Baltus GA, Kowalski MP, Tutter AV, Kadam S. 2009. A positive regulatory role for the mSin3A-HDAC complex in pluripotency through Nanog and Sox2. *J Biol Chem* **284**: 6998–7006. doi:10.1074/jbc.M807670200
- Barnes CE, English DM, Cowley SM. 2019. Acetylation & Co: an expanding repertoire of histone acylations regulates chromatin and transcription. *Essays Biochem* **63**: 97–107. doi:10.1042/EBC20180061
- Beconi M, Aziz O, Matthews K, Moumné L, O'Connell C, Yates D, Clifton S, Pett H, Vann J, Crowley L, et al. 2012. Oral administration of the pimelic diphenylamide HDAC inhibitor HDACi 4b is unsuitable for chronic inhibition of HDAC activity in the CNS in vivo. *PLoS One* **7**: e44498. doi:10.1371/journal.pone.0044498
- Bolger AM, Lohse M, Usadel B. 2014. Trimmomatic: a flexible trimmer for Illumina sequence data. *Bioinformatics* **30**: 2114–2120. doi:10.1093/bioinformatics/btu170
- Burgold T, Barber M, Kloet S, Cramard J, Gharbi S, Floyd R, Kinoshita M, Ralser M, Vermeulen M, Reynolds N, et al. 2019. The nucleosome remodelling and deacetylation complex suppresses transcriptional noise during lineage commitment. *EMBO J* **38**: e100788. doi:10.15252/embj.2018100788
- Chang HM, Paulson M, Holko M, Rice CM, Williams BR, Marié I, Levy DE. 2004. Induction of interferon-stimulated gene expression and antiviral responses require protein deacetylase activity. *Proc Natl Acad Sci* **101**: 9578–9583. doi:10.1073/pnas.0400567101
- Chen X, Xu H, Yuan P, Fang F, Huss M, Vega VB, Wong E, Orlov YL, Zhang W, Jiang J, et al. 2008. Integration of external signaling pathways with the core transcriptional network in embryonic stem cells. *Cell* **133**: 1106–1117. doi:10.1016/j.cell.2008.04.043
- Chen PB, Hung JH, Hickman TL, Coles AH, Carey JF, Weng Z, Chu F, Fazio TG. 2013. Hdac6 regulates Tip60-p400 function in stem cells. *eLife* **2**: e01557. doi:10.7554/eLife.01557
- Chou CJ, Herman D, Gottesfeld JM. 2008. Pimelic diphenylamide 106 is a slow, tight-binding inhibitor of class I histone deacetylases. *J Biol Chem* **283**: 35402–35409. doi:10.1074/jbc.M807045200
- Clayton AL, Hazzalin CA, Mahadevan LC. 2006. Enhanced histone acetylation and transcription: a dynamic perspective. *Mol Cell* **23**: 289–296. doi:10.1016/j.molcel.2006.06.017
- Core LJ, Martins AL, Danko CG, Waters CT, Siepel A, Lis JT. 2014. Analysis of nascent RNA identifies a unified architecture of initiation regions at mammalian promoters and enhancers. *Nat Genet* **46**: 1311–1320. doi:10.1038/ng.3142
- Di Micco R, Fontanals-Cirera B, Low V, Ntziachristos P, Yuen SK, Lovell CD, Dolgalev I, Yonekubo Y, Zhang G, Rusinova E, et al. 2014. Control of embryonic stem cell identity by BRD4-dependent transcriptional

- elongation of super-enhancer-associated pluripotency genes. *Cell Rep* **9**: 234–247. doi:10.1016/j.celrep.2014.08.055
- Dovey OM, Foster CT, Cowley SM. 2010a. Emphasizing the positive: a role for histone deacetylases in transcriptional activation. *Cell Cycle* **9**: 2700–2701. doi:10.4161/cc.9.14.12626
- Dovey OM, Foster CT, Cowley SM. 2010b. Histone deacetylase 1 (HDAC1), but not HDAC2, controls embryonic stem cell differentiation. *Proc Natl Acad Sci* **107**: 8242–8247. doi:10.1073/pnas.1000478107
- Dovey OM, Foster CT, Conte N, Edwards SA, Edwards JM, Singh R, Vassiliou G, Bradley A, Cowley SM. 2013. Histone deacetylase 1 and 2 are essential for normal T-cell development and genomic stability in mice. *Blood* **121**: 1335–1344. doi:10.1182/blood-2012-07-441949
- Fazio TG, Huff JT, Panning B. 2008. An RNAi screen of chromatin proteins identifies Tip60-p400 as a regulator of embryonic stem cell identity. *Cell* **134**: 162–174. doi:10.1016/j.cell.2008.05.031
- Finley LWS, Vardhana SA, Carey BW, Alonso-Curbelo D, Koche R, Chen Y, Wen D, King B, Radler MR, Rafii S, et al. 2018. Pluripotency transcription factors and Tet1/2 maintain Brd4-independent stem cell identity. *Nat Cell Biol* **20**: 565–574. doi:10.1038/s41556-018-0086-3
- Foster CT, Dovey OM, Lezina L, Luo JL, Gant TW, Barlev N, Bradley A, Cowley SM. 2010. Lysine-specific demethylase 1 regulates the embryonic transcriptome and CoREST stability. *Mol Cell Biol* **30**: 4851–4863. doi:10.1128/MCB.00521-10
- Gonzales-Cope M, Sidoli S, Bhanu NV, Won KJ, Garcia BA. 2016. Histone H4 acetylation and the epigenetic reader Brd4 are critical regulators of pluripotency in embryonic stem cells. *BMC Genomics* **17**: 95. doi:10.1186/s12864-016-2414-y
- Greer CB, Tanaka Y, Kim YJ, Xie P, Zhang MQ, Park IH, Kim TH. 2015. Histone deacetylases positively regulate transcription through the elongation machinery. *Cell Rep* **13**: 1444–1455. doi:10.1016/j.celrep.2015.10.013
- Gryder BE, Pomella S, Sayers C, Wu XS, Song Y, Chiarella AM, Bagchi S, Chou HC, Sinniah RS, Walton A, et al. 2019a. Histone hyperacetylation disrupts core gene regulatory architecture in rhabdomyosarcoma. *Nat Genet* **51**: 1714–1722. doi:10.1038/s41588-019-0534-4
- Gryder BE, Wu L, Woldemichael GM, Pomella S, Quinn TR, Park PMC, Cleveland A, Stanton BZ, Song Y, Rota R, et al. 2019b. Chemical genomics reveals histone deacetylases are required for core regulatory transcription. *Nat Commun* **10**: 3004. doi:10.1038/s41467-019-11046-7
- Haberland M, Montgomery RL, Olson EN. 2009. The many roles of histone deacetylases in development and physiology: implications for disease and therapy. *Nat Rev Genet* **10**: 32–42. doi:10.1038/nrg2485
- Horne GA, Stewart HJ, Dickson J, Knapp S, Ramsahoye B, Chevassut T. 2015. Nanog requires BRD4 to maintain murine embryonic stem cell pluripotency and is suppressed by bromodomain inhibitor JQ1 together with Lefty1. *Stem Cells Dev* **24**: 879–891. doi:10.1089/scd.2014.0302
- Jacobson RH, Ladurner AG, King DS, Tjian R. 2000. Structure and function of a human TAF₂₅₀ double bromodomain module. *Science* **288**: 1422–1425. doi:10.1126/science.288.5470.1422
- Jamaladdin S, Kelly RD, O'Regan L, Dovey OM, Hodson GE, Millard CJ, Portolano N, Fry AM, Schwabe JW, Cowley SM. 2014. Histone deacetylase (HDAC) 1 and 2 are essential for accurate cell division and the pluripotency of embryonic stem cells. *Proc Natl Acad Sci* **111**: 9840–9845. doi:10.1073/pnas.1321330111
- Jang MK, Mochizuki K, Zhou M, Jeong HS, Brady JN, Ozato K. 2005. The bromodomain protein Brd4 is a positive regulatory component of P-TEFb and stimulates RNA polymerase II-dependent transcription. *Mol Cell* **19**: 523–534. doi:10.1016/j.molcel.2005.06.027
- Kaji K, Caballero IM, MacLeod R, Nichols J, Wilson VA, Hendrich B. 2006. The NuRD component Mbd3 is required for pluripotency of embryonic stem cells. *Nat Cell Biol* **8**: 285–292. doi:10.1038/ncb1372
- Kanno T, Kanno Y, Siegel RM, Jang MK, Lenardo MJ, Ozato K. 2004. Selective recognition of acetylated histones by bromodomain proteins visualized in living cells. *Mol Cell* **13**: 33–43. doi:10.1016/S1097-2765(03)00482-9
- Kanno T, Kanno Y, LeRoy G, Campos E, Sun HW, Brooks SR, Vahedi G, Heightman TD, Garcia BA, Reinberg D, et al. 2014. BRD4 assists elongation of both coding and enhancer RNAs by interacting with acetylated histones. *Nat Struct Mol Biol* **21**: 1047–1057. doi:10.1038/nsmb.2912
- Karantzi E, Schulz H, Hummel O, Hubner N, Hatzopoulos A, Kretsovali A. 2008. Histone deacetylase inhibition accelerates the early events of stem cell differentiation: transcriptomic and epigenetic analysis. *Genome Biol* **9**: R65. doi:10.1186/gb-2008-9-4-r65
- Kelly RD, Cowley SM. 2013. The physiological roles of histone deacetylase (HDAC) 1 and 2: complex co-stars with multiple leading parts. *Biochem Soc Trans* **41**: 741–749. doi:10.1042/BST20130010
- Kelly RDW, Chandru A, Watson PJ, Song Y, Blades M, Robertson NS, Jamieson AG, Schwabe JWR, Cowley SM. 2018. Histone deacetylase (HDAC) 1 and 2 complexes regulate both histone acetylation and crotonylation in vivo. *Sci Rep* **8**: 14690. doi:10.1038/s41598-018-32927-9
- Kidder BL, Palmer S. 2012. HDAC1 regulates pluripotency and lineage specific transcriptional networks in embryonic and trophoblast stem cells. *Nucleic Acids Res* **40**: 2925–2939. doi:10.1093/nar/gkr1151
- Kim TK, Hemberg M, Gray JM, Costa AM, Bear DM, Wu J, Harmin DA, Laptewicz M, Barbara-Haley K, Kuersten S, et al. 2010. Widespread transcription at neuronal activity-regulated enhancers. *Nature* **465**: 182–187. doi:10.1038/nature09033
- Kim YJ, Greer CB, Cecchini KR, Harris LN, Tuck DP, Kim TH. 2013. HDAC inhibitors induce transcriptional repression of high copy number genes in breast cancer through elongation blockade. *Oncogene* **32**: 2828–2835. doi:10.1038/onc.2013.32
- Kwak H, Fuda NJ, Core LJ, Lis JT. 2013. Precise maps of RNA polymerase reveal how promoters direct initiation and pausing. *Science* **339**: 950–953. doi:10.1126/science.1229386
- Langmead B, Salzberg SL. 2012. Fast gapped-read alignment with Bowtie 2. *Nat Methods* **9**: 357–359. doi:10.1038/nmeth.1923
- Laubach JP, Moreau P, San-Miguel JF, Richardson PG. 2015. Panobinostat for the treatment of multiple myeloma. *Clin Cancer Res* **21**: 4767–4773. doi:10.1158/1078-0432.CCR-15-0530
- Lauffer BE, Mintzer R, Fong R, Mukund S, Tam C, Zilberleyb I, Flicke B, Ritscher A, Fedorowicz G, Vallero R, et al. 2013. Histone deacetylase (HDAC) inhibitor kinetic rate constants correlate with cellular histone acetylation but not transcription and cell viability. *J Biol Chem* **288**: 26926–26943. doi:10.1074/jbc.M113.490706
- Liu W, Stein P, Cheng X, Yang W, Shao NY, Morrisey EE, Schultz RM, You J. 2014. BRD4 regulates Nanog expression in mouse embryonic stem cells and preimplantation embryos. *Cell Death Differ* **21**: 1950–1960. doi:10.1038/cdd.2014.124
- Luger K, Richmond TJ. 1998. The histone tails of the nucleosome. *Curr Opin Genet Dev* **8**: 140–146. doi:10.1016/S0959-437X(98)80134-2
- Martello G, Smith A. 2014. The nature of embryonic stem cells. *Annu Rev Cell Dev Biol* **30**: 647–675. doi:10.1146/annurev-cellbio-100913-013116
- Métivier R, Penot G, Hubner MR, Reid G, Brand H, Kos M, Gannon F. 2003. Estrogen receptor- α directs ordered, cyclical, and combinatorial recruitment of cofactors on a natural target promoter. *Cell* **115**: 751–763. doi:10.1016/S0092-8674(03)00934-6
- Millard CJ, Watson PJ, Fairall L, Schwabe JW. 2017. Targeting class I histone deacetylases in a “complex” environment. *Trends Pharmacol Sci* **38**: 363–377. doi:10.1016/j.tips.2016.12.006
- Mootha VK, Lindgren CM, Eriksson KF, Subramanian A, Sihag S, Lehar J, Puigserver P, Carlsson E, Riddlerstale M, Laurila E, et al. 2003. PGC-1 α -responsive genes involved in oxidative phosphorylation are coordinately downregulated in human diabetes. *Nat Genet* **34**: 267–273. doi:10.1038/ng1180
- Nagy L, Kao HY, Chakravarti D, Lin RJ, Hassig CA, Ayer DE, Schreiber SL, Evans RM. 1997. Nuclear receptor repression mediated by a complex containing SMRT, mSin3A, and histone deacetylase. *Cell* **89**: 373–380. doi:10.1016/S0092-8674(00)80218-4
- Preker P, Nielsen J, Kammler S, Lykke-Andersen S, Christensen MS, Mampandano CK, Schierup MH, Jensen TH. 2008. RNA exosome depletion reveals transcription upstream of active human promoters. *Science* **322**: 1851–1854. doi:10.1126/science.1164096
- Quinlan AR, Hall IM. 2010. BEDTools: a flexible suite of utilities for comparing genomic features. *Bioinformatics* **26**: 841–842. doi:10.1093/bioinformatics/btq033
- Robinson PJ, An W, Routh A, Martino F, Chapman L, Roeder RG, Rhodes D. 2008. 30nm chromatin fibre decompaction requires both H4-K16 acetylation and linker histone eviction. *J Mol Biol* **381**: 816–825. doi:10.1016/j.jmb.2008.04.050
- Robinson JT, Thorvaldsdóttir H, Winckler W, Guttman M, Lander ES, Getz G, Mesirov JP. 2011. Integrative genomics viewer. *Nat Biotechnol* **29**: 24–26. doi:10.1038/nbt.1754
- Sakamoto S, Potla R, Larner AC. 2004. Histone deacetylase activity is required to recruit RNA polymerase II to the promoters of selected interferon-stimulated early response genes. *J Biol Chem* **279**: 40362–40367. doi:10.1074/jbc.M406400200
- Sanchez GJ, Richmond PA, Bunker EN, Karman SS, Azoifeifa J, Garnett AT, Xu Q, Wheeler GE, Toomey CM, Zhang Q, et al. 2018. Genome-wide dose-dependent inhibition of histone deacetylases studies reveal their roles in enhancer remodeling and suppression of oncogenic super-enhancers. *Nucleic Acids Res* **46**: 1756–1776. doi:10.1093/nar/gkx1225
- Saunders A, Core LJ, Lis JT. 2006. Breaking barriers to transcription elongation. *Nat Rev Mol Cell Biol* **7**: 557–567. doi:10.1038/nrm1981
- Simandi Z, Horvath A, Wright LC, Cuaranta-Monroy I, De Luca I, Karolyi K, Sauer S, Deleuze JF, Gudas LJ, Cowley SM, et al. 2016. OCT4 acts as an integrator of pluripotency and signal-induced differentiation. *Mol Cell* **63**: 647–661. doi:10.1016/j.molcel.2016.06.039
- Smith CL. 2008. A shifting paradigm: histone deacetylases and transcriptional activation. *Bioessays* **30**: 15–24. doi:10.1002/bies.20687
- Stengel KR, Barnett KR, Wang J, Liu Q, Hodges E, Hiebert SW, Bhaskara S. 2017. Deacetylase activity of histone deacetylase 3 is required for

- productive VDJ recombination and B-cell development. *Proc Natl Acad Sci* **114**: 8608–8613. doi:10.1073/pnas.1701610114
- Stojanovic N, Hassan Z, Wirth M, Wenzel P, Beyer M, Schäfer C, Brand P, Kroemer A, Stauber RH, Schmid RM, et al. 2017. HDAC1 and HDAC2 integrate the expression of p53 mutants in pancreatic cancer. *Oncogene* **36**: 1804–1815. doi:10.1038/onc.2016.344
- Streubel G, Fitzpatrick DJ, Oliviero G, Scelfo A, Moran B, Das S, Munawar N, Watson A, Wynne K, Negri GL, et al. 2017. Fam60a defines a variant Sin3a-Hdac complex in embryonic stem cells required for self-renewal. *EMBO J* **36**: 2216–2232. doi:10.15252/embj.201696307
- Subramanian A, Tamayo P, Mootha VK, Mukherjee S, Ebert BL, Gillette MA, Paulovich A, Pomeroy SL, Golub TR, Lander ES, et al. 2005. Gene set enrichment analysis: a knowledge-based approach for interpreting genome-wide expression profiles. *Proc Natl Acad Sci* **102**: 15545–15550. doi:10.1073/pnas.0506580102
- Turnbull RE, Fairall L, Saleh A, Kelsall E, Morris KL, Ragan TJ, Savva CG, Chandru A, Millard CJ, Makarova OV, et al. 2020. The MiDAC histone deacetylase complex is essential for embryonic development and has a unique multivalent structure. *Nat Commun* **11**: 3252. doi:10.1038/s41467-020-17078-8
- Vaid R, Wen J, Mannervik M. 2020. Release of promoter-proximal paused Pol II in response to histone deacetylase inhibition. *Nucleic Acids Res* **48**: 4877–4890. doi:10.1093/nar/gkaa234
- Verdin E, Ott M. 2015. Fifty years of protein acetylation: from gene regulation to epigenetics, metabolism and beyond. *Nat Rev Mol Cell Biol* **16**: 258–264. doi:10.1038/nrm3931
- Wang Z, Zang C, Cui K, Schonnes DE, Barski A, Peng W, Zhao K. 2009. Genome-wide mapping of HATs and HDACs reveals distinct functions in active and inactive genes. *Cell* **138**: 1019–1031. doi:10.1016/j.cell.2009.06.049
- Wang J, Zhao Y, Zhou X, Hiebert SW, Liu Q, Shyr Y. 2018. Nascent RNA sequencing analysis provides insights into enhancer-mediated gene regulation. *BMC Genomics* **19**: 633. doi:10.1186/s12864-018-5016-z
- Watson PJ, Fairall L, Santos GM, Schwabe JW. 2012. Structure of HDAC3 bound to co-repressor and inositol tetraphosphate. *Nature* **481**: 335–340. doi:10.1038/nature10728
- Weinert BT, Narita T, Satpathy S, Srinivasan B, Hansen BK, Schözl C, Hamilton WB, Zucconi BE, Wang WW, Liu WR, et al. 2018. Time-resolved analysis reveals rapid dynamics and broad scope of the CBP/p300 acetylome. *Cell* **174**: 231–244.e12. doi:10.1016/j.cell.2018.04.033
- Whyte WA, Bilodeau S, Orlando DA, Hoke HA, Frampton GM, Foster CT, Cowley SM, Young RA. 2012. Enhancer decommissioning by LSD1 during embryonic stem cell differentiation. *Nature* **482**: 221–225. doi:10.1038/nature10805
- Whyte WA, Orlando DA, Hnisz D, Abraham BJ, Lin CY, Kagey MH, Rahl PB, Lee TI, Young RA. 2013. Master transcription factors and mediator establish super-enhancers at key cell identity genes. *Cell* **153**: 307–319. doi:10.1016/j.cell.2013.03.035
- Wu T, Pinto HB, Kamikawa YF, Donohoe ME. 2015. The BET family member BRD4 interacts with OCT4 and regulates pluripotency gene expression. *Stem Cell Reports* **4**: 390–403. doi:10.1016/j.stemcr.2015.01.012
- Yang Z, Yik JH, Chen R, He N, Jang MK, Ozato K, Zhou Q. 2005. Recruitment of P-TEFb for stimulation of transcriptional elongation by the bromodomain protein Brd4. *Mol Cell* **19**: 535–545. doi:10.1016/j.molcel.2005.06.029
- Zhao Y, Liu Q, Acharya P, Stengel KR, Sheng Q, Zhou X, Kwak H, Fischer MA, Bradner JE, Strickland SA, et al. 2016. High-resolution mapping of RNA polymerases identifies mechanisms of sensitivity and resistance to BET inhibitors in t(8;21) AML. *Cell Rep* **16**: 2003–2016. doi:10.1016/j.celrep.2016.07.032
- Zhu F, Zhu Q, Ye D, Zhang Q, Yang Y, Guo X, Liu Z, Jiapaer Z, Wan X, Wang G, et al. 2018. Sin3a-Tet1 interaction activates gene transcription and is required for embryonic stem cell pluripotency. *Nucleic Acids Res* **46**: 6026–6040. doi:10.1093/nar/gky347
- Zupkovitz G, Tischler J, Posch M, Sadzak I, Ramsauer K, Egger G, Grausenburger R, Schweifer N, Chiocia S, Decker T, et al. 2006. Negative and positive regulation of gene expression by mouse histone deacetylase 1. *Mol Cell Biol* **26**: 7913–7928. doi:10.1128/MCB.01220-06

Received April 28, 2023; accepted in revised form December 20, 2023.